

Microfabricated PCR-electrochemical device for simultaneous DNA amplification and detection

Thomas Ming-Hung Lee,^a Maria C. Carles^b and I-Ming Hsing^{*ab}

^a Department of Chemical Engineering, Hong Kong University of Science and Technology, Clear Water Bay, Kowloon, Hong Kong SAR. E-mail: kehsing@ust.hk; Fax: +(852) 23580054; Tel: +(852) 23587131

^b Bioengineering Graduate Program, Hong Kong University of Science and Technology, Clear Water Bay, Kowloon, Hong Kong SAR

Received 20th January 2003, Accepted 25th March 2003
First published as an Advance Article on the web 17th April 2003

Microfabricated silicon/glass-based devices with functionalities of simultaneous polymerase chain reaction (PCR) target amplification and sequence-specific electrochemical (EC) detection have been successfully developed. The microchip-based device has a reaction chamber (volume of 8 μ l) formed in a silicon substrate sealed by bonding to a glass substrate. Electrode materials such as gold and indium tin oxide (ITO) were patterned on the glass substrate and served as EC detection platforms where DNA probes were immobilized. Platinum temperature sensors and heaters were patterned on top of the silicon substrate for real-time, precise and rapid thermal cycling of the reaction chamber as well as for efficient target amplification by PCR. DNA analyses in the integrated PCR-EC microchip start with the asymmetric PCR amplification to produce single-stranded target amplicons, followed by immediate sequence-specific recognition of the PCR product as they hybridize to the probe-modified electrode. Two electrochemistry-based detection techniques including metal complex intercalators and nanogold particles are employed in the microdevice to achieve a sensitive detection of target DNA analytes. With the integrated PCR-EC microdevice, the detection of trace amounts of target DNA (as few as several hundred copies) is demonstrated. The ability to perform DNA amplification and EC sequence-specific product detection simultaneously in a single reaction chamber is a great leap towards the realization of a truly portable and integrated DNA analysis system.

1 Introduction

The development of micro-analytical devices has brought revolutionary changes to the area of deoxyribonucleic acid (DNA) assays.^{1,2} These micro-scale analyzers not only benefit from the reduction in sample/reagent volumes but also the enhanced analytical performance (e.g., speed and sensitivity). Most importantly, miniaturization offers the opportunity to integrate all functional steps of the DNA analysis into a single microchip-based device.^{3,4} This integrated micro-total analytical system (μ -TAS) permits full automation, thereby minimizing sample contamination from manual operation. The great interest in developing a portable DNA analyzer is targeted for decentralized screening of pathogens in food, water and environment as well as for clinical diagnosis. Such a hand-held device should ideally encompass all steps from sample preparation, target amplification to amplicon detection.

DNA amplification by the polymerase chain reaction (PCR)⁵ is an indispensable tool in routine DNA assays, particularly when rare targets are being tested. Significant studies have been carried out to develop effective and reliable microchip-based PCR devices.^{6–12} Over the past few years, different degrees of integration with the micro-PCR module, including upstream sample preparation¹³ or downstream PCR product detection,^{14–19} have been successfully demonstrated. To date, only a limited number of sophisticated microfluidic devices, which are capable of automatically metering and mixing sample/reagent solutions, amplifying target DNA and detecting the PCR product, have been reported.^{4,20,21}

In recent years, attempts have been made to run PCR directly from crude blood and cell samples,^{21,22} lessening the need to integrate the sample preparation functionality with the micro-PCR module. The bottleneck delaying the realization of a truly

integrated DNA analyzer is a portable detection module for on-chip PCR product detection. The most common detection scheme requires capillary electrophoretic separation of the PCR product (along with molecular weight markers), followed by laser-excited fluorescence detection.^{16–19} However, optical systems are difficult to miniaturize onto a monolithic micro-analytical system. Towards the goal of achieving a fully integrated DNA microchip, alternative microfabrication-compatible detection techniques have to be sought for. Electrochemical (EC) method, with its inherent advantages of miniaturization and high sensitivity, has long been utilized for detecting DNA molecules.²³ Another feature of the EC DNA detection is the ability to obtain sequence information. This is accomplished by exploiting the hybridization between DNA probe (oligonucleotide complementary to the target sequence) immobilized on an electrode transducer surface and target analyte. The EC transduction of the hybridization event relies typically on external electrochemically-active indicators, which comprise DNA intercalators (metal complexes,^{24,25} anthracycline antibiotics,²⁶ and bisbenzimidazole dyes^{27,28}), enzymes,^{29,30} and metal nanoparticles.^{31–33} Despite the extensive research efforts in EC hybridization transduction, just a few groups,^{28,29,34} including our group, have devoted to PCR product detection. Moreover, to the best of our knowledge, the integration of microchip-based PCR with EC detection functionality has not been reported yet.

In a previous study, we demonstrated DNA amplification in a silicon/glass-based PCR microreactor.¹² Later on, we successfully expanded the capability of the microdevice for *in situ* PCR product detection via a DNA microarray integrated onto the PCR reaction chamber.³ Nevertheless, the detection was still hinged on fluorescence microscopy. In this paper, we report on the development of an integrated PCR-EC microdevice for

simultaneous DNA amplification, detection and quantitation. The microdevice consists of a reaction chamber formed in a silicon substrate, and an EC sensor fabricated onto a glass substrate. Heaters and temperature sensors are patterned on top of the reaction chamber for thermal cycling of PCR. The glass substrate serves as not only a seal for the reaction chamber but also a platform for the EC detection of the PCR product. Here, both the amplification of the target DNA sequence and the subsequent EC detection of the PCR product are carried out inside the reaction chamber. Sequence-specific recognition of the target analyte is achieved through hybridization with the probe immobilized onto the working electrode on the glass substrate. Building on our experience in the intercalator-based approach for the EC hybridization transduction with gold electrode,²⁸ its implementation in the integrated PCR-EC device for a sensitive and selective DNA assay is presented. To demonstrate the capability of this microchip format in adapting different EC transduction schemes, the intercalator-based approach is replaced with a silver-enhanced gold nanoparticle approach.^{35,36} In the latter approach, silver metal is catalytically deposited onto gold nanoparticles (hybridization label) and then oxidized electrochemically to obtain the analytical signal.

2 Experimental

2.1 Reagents

Four oligonucleotides were purchased from Synthetic Genetics (San Diego, CA) with the following base sequences: 5'-CAC AAA ACG GGG GCG G-3' (forward primer), same base sequence as the forward primer but modified with a mercaptohexyl group at the 5' end (probe), 5'-GGA TTC TTA GTG CTG GTA TGA TCG CA-3' (reverse primer), one with and the other one without a biotin group at the 5' end. All other PCR reagents were purchased from Invitrogen (Carlsbad, CA), unless otherwise stated.

Sodium chloride, sodium dihydrogen phosphate, disodium hydrogen phosphate, trisodium citrate dihydrate and sodium nitrate were acquired from RdH (Sigma-Aldrich, Germany). Bovine serum albumin (BSA), hydrochloric acid (38%), streptavidin-colloidal gold (10 nm), silver enhancement kit were obtained from Sigma (St. Louis, MO). Hoechst 33258 was purchased from Arcos Organics (Belgium). Alconox, propan-2-ol, ammonium hydroxide (30%) and (3-mercaptopropyl)trimethoxysilane (MPTS) were purchased from Aldrich (Milwaukee, WI). All solutions were prepared with ultra-pure water from a Millipore Milli-Q system.

2.2 Device fabrication

The polymerase chain reaction-electrochemical (PCR-EC) microchip is composed of silicon and glass substrates. A reaction chamber (dimensions of 5.8 mm (L) × 3.7 mm (W) × 0.35 mm (H), the length and width are reported at half depth) was formed in the silicon substrate with a bottom glass substrate sealing the chamber. Platinum temperature sensors and heaters are integrated on top of the silicon substrate for real-time temperature monitoring and control. The glass substrate also functions as a detection platform, where electrodes for the EC measurements are patterned on its surface.

The fabrication of the silicon substrate was according to our previously reported procedure¹² with slight modifications. In brief, a silicon wafer (double-side polished, <100> and 400 μm thick) was coated with SiO₂ and low-stress silicon nitride (Si_xN_y) by thermal oxidation and low-pressure chemical vapor deposition, respectively. Then, photolithography was used to define the reaction chamber geometry on the bottom side of the wafer. Plasma etching was employed to remove the exposed

Si_xN_y, followed by buffered oxide etch to remove the underlying oxide. Immediately after this, KOH etching was performed to create the 350 μm deep reaction chamber. The remaining Si_xN_y was removed and an additional oxide layer was grown to passivate the chamber wall. The platinum temperature sensors and heaters were patterned on top of the wafer using a lift-off process.

Two types of glass substrates were used in this work: Corning 7740 (Corning, NY) and indium tin oxide (ITO)-coated (Delta Technologies, Stillwater, MN) glasses for the intercalator (Hoechst 33258) and gold nanoparticle-based experiments, respectively. Corning 7740 glass electrodes (gold working electrode, platinum counter and pseudo-reference electrodes) were patterned on the surface by a lift-off process. Two holes were drilled onto the glass for reagent injection into the PCR reaction chamber. An improved anodic bonding technique³⁷ developed in our group was employed to seal the reaction chamber with the Corning 7740 glass while UV-curing glue (Summers Optical, Fort Washington, PA) was used with the ITO glass. The ITO glass had to undergo some cleaning and pretreatment steps prior to the bonding process. It was sequentially sonicated in an Alconox solution (8 g of Alconox/L of water), propan-2-ol, and water (twice), 15 minutes each. Then, it was immersed in a 1% NH₄OH solution at 80 °C for 1 hour, and rinsed thoroughly with water. The ITO surface was modified with a self-assembled monolayer of MPTS by incubating in a solution containing 10 mL of propan-2-ol, 250 μL of MPTS, and 100 μL of H₂O at 80 °C for 30 minutes, followed by propan-2-ol and water rinsing.

The working electrodes (gold and ITO electrodes) of the assembled PCR-EC microdevices were modified with the probe for subsequent target recognition after the PCR. This was achieved by filling the reaction chamber with 25 μM of the probe solution (500 mM NaCl/25 mM Na phosphate, pH 7.0) and allowing the coupling reaction to proceed for 24 hours at room temperature. Finally, the probe solution was pipetted out, and the reaction chamber was flushed with copious amounts of water to remove any non-specifically adsorbed probe molecules.

2.3 Instrumentation

The setup for a DNA analysis with the PCR-EC microdevice consists of the following components: analytical prober, data acquisition system, digital control unit, power supply, and electrochemical system. The analytical prober (Karl Suss, Germany) was used to align heater and temperature sensor contact pads of the PCR-EC microdevice to a customized probe card for electrical connection between the chip and external electronic components. The temperature sensors were connected to a data acquisition (DAQ) card (PCI-MIO-16E-1, National Instruments, Austin, TX) through a signal conditioning board (SC-2042-RTD, National Instruments), which gave the temperature sensors an excitation current of 1 mA. The conversion from voltage reading to temperature was based on a calibration plot of sensor's resistance against temperature as described in the Results and discussion section. A digital feedback proportional-integral-derivative (PID) with gain scheduling control algorithm^{12,38} was implemented in LabVIEW (National Instruments) to control voltage supply to the heater by an external power source (HP6629A, Hewlett-Packard, Rockville, MD).

Electrochemical measurements with the differential pulse voltammetry and linear sweep voltammetry techniques were performed using an Autolab PGSTAT 30 potentiostat/galvanostat (Eco Chemie, The Netherlands) controlled by the General Purpose Electrochemical System (GPES 4.8) software (Eco Chemie). For the PCR-EC chip with ITO as the working electrode, a platinum wire counter electrode and a Ag/AgCl

reference electrode (immersed in a 3 M NaCl filling solution saturated with AgCl, EG&G, Princeton Applied Research, Oak Ridge, TN) were used.

2.4 Assay protocol

For each experiment, 10 μl PCR-mix was prepared. The mixture contains 1 μl of $10 \times$ PCR buffer solution (200 mM Tris-HCl, pH 8.4, 500 mM KCl), 0.4 μl of 50 mM MgCl_2 , 0.2 μl of 10 mM dNTPs, 0.4 μl of 0.1 μM forward primer, 0.4 μl of 10 μM reverse primer, 0.25 μl of 20 $\mu\text{g}/\mu\text{l}$ BSA, 0.4 μl of 1 ng/ μl DNA template, 0.1 μl of 5 U/ μl Taq DNA polymerase, and 6.85 μl of autoclaved double-deionized water. Note that the non-biotinylated reverse primer was used for the intercalator-based experiments while the biotinylated one was for the gold nanoparticle-based experiments. The DNA template consists of the 5S-rRNA spacer gene of the traditional Chinese medicinal herb *Fritillaria thunbergii*³⁹ (~600 bp) cloned into pCR^{2.1}-TOPO[®] TA vector (3.9 kbp). The mastermix was subjected to the following thermal cycling profile inside the reaction chamber of the PCR-EC microdevice: initial denaturation at 95 $^{\circ}\text{C}$ for 5 minutes, 40 cycles at 95 $^{\circ}\text{C}$ for 30 seconds, at 55 $^{\circ}\text{C}$ for 30 seconds, at 72 $^{\circ}\text{C}$ for 30 seconds, and a final extension at 72 $^{\circ}\text{C}$ for 5 minutes.

After the asymmetric PCR, the reaction chamber was cooled back to ambient temperature within a short period of time (1 minute). The reaction mixture was incubated for 1 hour, allowing the PCR product to hybridize with the probe immobilized onto the working electrode. The reaction chamber was then rinsed with large quantities of washing buffer (300 mM NaCl/30 mM Na citrate, pH 7.0, $2 \times$ SSC buffer) to get rid of any unhybridized products. For the PCR-EC device with gold working electrode, signal transduction of the hybridization event was based on the DNA intercalator. This was simply done by introducing a 100 μM Hoechst 33258 solution (100 mM NaCl/10 mM Na phosphate, pH 7.0) into the reaction chamber for 5 minutes, followed by differential pulse voltammetric scan of the gold electrode from +0.2 V to +0.8 V at a scan rate of 100 mV s^{-1} . For the PCR-EC device with ITO working electrode, the gold nanoparticle hybridization label was bound to the hybridized PCR product *via* biotin-streptavidin interaction (incubation time of 1 hour). Non-specifically bound gold nanoparticles were washed off with 0.3 M NaNO_3 /10 mM Na phosphate (pH 7.0) buffer. Then, silver deposition was performed in accordance with the manufacturer's instruction. The duration of the silver enhancement was set to 8 minutes. After that, the reaction chamber was rinsed with water to remove the silver enhancement solution. The amount of silver deposited onto the gold nanoparticle label was determined by measuring the oxidative silver dissolution current during a linear sweep voltammetric scan. The measurements were conducted at a scan rate of 100 mV s^{-1} with 0.1 M KNO_3 as the supporting electrolyte.

3 Results and discussion

The integrated polymerase chain reaction-electrochemical (PCR-EC) microdevice has a reaction chamber volume of ~8 μl . The microchip has integrated temperature sensors and heaters for accurate thermal cycling of the reaction chamber for the PCR. An expanded schematic illustration of the pattern of the temperature sensors and heaters is given in Fig. 1A. The average temperature reading of the two sensors on the left (S1 and S2) is used to control the left heater (H1) while S3/S4 and H2 form the other pair. Fig. 1B shows the bottom and cross-sectional views of the anodically bonded PCR-EC device with gold working electrode.

In a previous study, we have successfully demonstrated the functional integration of PCR and DNA microarrays with fluorescence detection in the same reaction chamber.³ Here, aiming at developing a truly portable DNA analysis system, the optical detection system is substituted by the electrochemical system. With experience in the sequence-specific electrochemical detection of PCR product using the intercalator-based approach,²⁸ it is desirable to implement the same detection methodology in the prototypical PCR-EC microdevice. Gold is a good choice of working electrode material for three main reasons: (1) it can be easily patterned on the glass substrate using the lift-off process; (2) the DNA probe can be readily immobilized onto the gold surface *via* thiol chemisorption (the probe is modified with a thiol group at the 5' end), and the bonding is strong enough to resist the denaturation temperature of the PCR; (3) the background electrochemical signal resulting from the non-specific adsorption of the intercalator onto the gold electrode surface is reasonably low.

The assembled PCR-EC microdevice with gold working electrode modified with the probe can now be utilized for a DNA assay with simultaneous DNA amplification and electrochemical product detection. Fig. 2 depicts the basic assay principle with the PCR-EC microchip. First, the PCR reaction mixture containing the DNA analyte is applied to the reaction chamber (Fig. 2A). Second, the reaction chamber is thermally cycled by the heaters integrated on top of the silicon substrate to amplify the target DNA sequence. In our PCR protocol, one primer (the reverse primer) is supplied in large excess (100-fold) over the other one (the forward primer) so that single-stranded rich target amplicon is produced (Fig. 2B). With this, there is no need to heat denature the double-stranded PCR product (typical of normal PCR) for the subsequent hybridization process. Besides, the possibility of reannealing of the denatured PCR product, which may lower the hybridization efficiency and reproducibility with the probe, is eliminated. Third, the single-stranded PCR amplicon will hybridize with the probe immobilized on the working electrode surface if a certain region of the amplified sequence is complementary to the probe (Fig. 2C). Finally, the hybridization indicator (either Hoechst 33258 or gold nanoparticle in this work) is bound to the hybridized amplicon, the amount of which is electrochemically determined (Fig. 2D).

Prior to the discussions on the electrochemical detection of the PCR product within the PCR reaction chamber, some points concerning the thermal characteristics and surface chemistries of the PCR-EC devices have to be addressed. The degree of precision on the temperature control of the PCR reaction chamber is related to the accuracy in establishing the sensor's resistance-temperature correlation curve:

$$R = R_0(1 + \alpha(T - T_0))$$

where R and R_0 are resistances of the temperature sensor at temperatures T and T_0 (reference temperature), and α is the temperature coefficient of resistance (TCR). This equation is used in converting the voltage reading (from the temperature sensors connected to the signal conditioning board that provides a constant excited current of 1 mA) to the temperature reading. When R is plotted against T , a linear graph with a regression coefficient of 0.9996 is obtained. The slope of this linear graph gives a TCR value of $1.75 \times 10^{-3}/^{\circ}\text{C}$. With the well-calibrated temperature sensors and proper tuning of the digital proportional-integral-derivative (PID) control for the heaters, temperature precision of ± 0.025 $^{\circ}\text{C}$ and fast thermal cycling (heating and cooling rates of 5 and 3.5 $^{\circ}\text{C s}^{-1}$, respectively) of the PCR reaction chamber are achieved.¹²

One key issue for the microfabricated PCR device is the surface chemistry of the reaction chamber. To ensure an efficient DNA amplification in the silicon-based microdevice, the reaction chamber has to be passivated with a thin layer of silicon oxide, as shown in Fig. 1B (the right diagram).^{7,12} Besides surface passivation of the silicon-side reaction cham-

ber, attention should also be given to the surface chemistry of the glass substrate within the reaction chamber. Properties of both glass surfaces (Corning 7740 glass and MPTS-modified ITO glass) in our PCR-EC microdevices are compatible with PCR reaction. This was confirmed by similar PCR amplification performances in the microdevice and conventional thermal cycler (data not shown).

The capability to identify the presence of a specific DNA sequence using the PCR-EC microdevice (gold working electrode) with the intercalator-based approach is demonstrated in Fig. 3. When the target DNA template is present, then the asymmetric PCR amplicon hybridizes with the probe immobilized onto the gold working electrode surface. The formed hybrid bears more intercalator molecules than the probe due to

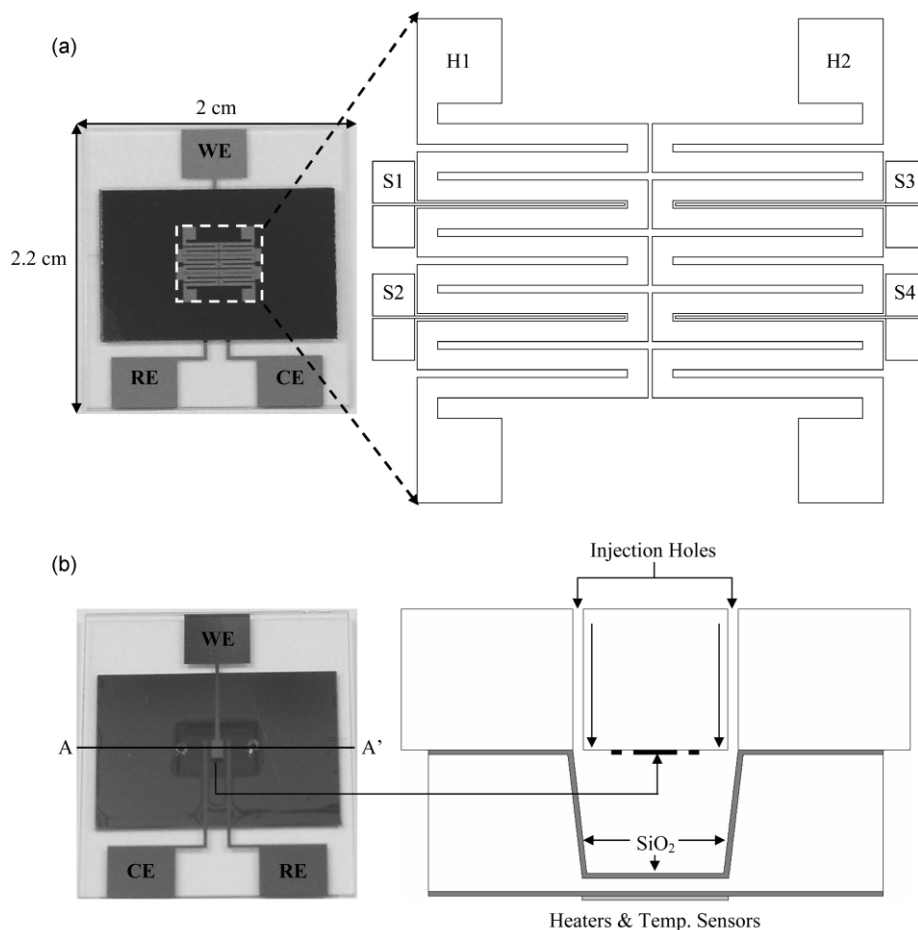


Fig. 1 Photographs showing the integrated polymerase chain reaction-electrochemical (PCR-EC) microdevice: (a) top view of the PCR-EC microchip with schematic representation of the platinum heaters (H1 and H2) and temperature sensors (S1–S4); (b) bottom and cross-sectional (indicated by the line AA') views of the PCR-EC microchip. Note that WE, RE and CE are the working, reference, and counter electrodes of the electrochemical sensor, respectively.

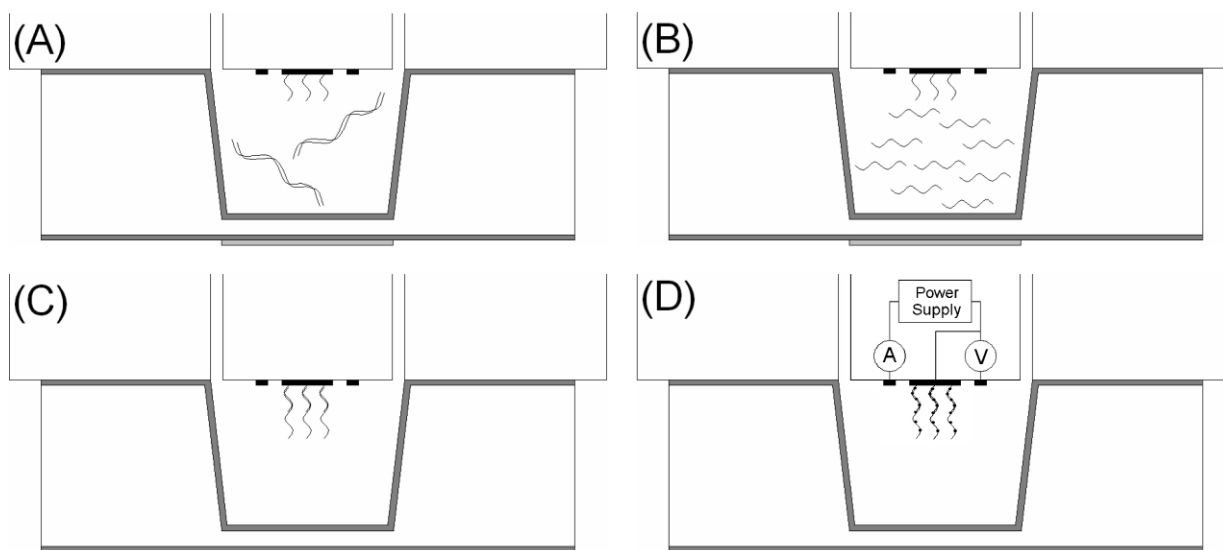


Fig. 2 A diagram depicting the assay principle of the integrated PCR-EC microdevice. (A) PCR-mix containing the DNA analyte is loaded into the reaction chamber; (B) Asymmetric PCR is carried out to produce single-stranded rich target amplicon; (C) Hybridization of the target amplicon to the probe immobilized on the working electrode; (D) Binding of the electrochemically-active hybridization indicator and electrochemical transduction.

the fact that the intercalator preferentially binds to double-stranded hybrid rather than to single-stranded DNA. In addition, the formed hybrid (only the region that binds to the probe is double-stranded, 16-mer) has a long single-stranded tail (~ 400 bases) that incorporates a lot more intercalator molecules than that of the probe. Therefore, there is a significant pre-concentration of the electrochemically active intercalator molecules close to the electrode surface, resulting in an enhanced oxidation current peak of the Hoechst 33258 (solid curve of Fig. 3). A series of experiments with varying amounts of the target DNA template are performed. A plot of the peak current of the intercalator (Hoechst 33258) during differential pulse voltammetry against log of number of copies of the DNA template in the PCR reaction chamber is given in Fig. 4. The fitted correlation curve is sigmoidal in shape, and indicates a detection limit of a few hundreds of the template molecules (template concentration of less than $0.4 \text{ fg } \mu\text{l}^{-1}$).

To demonstrate the flexibility of this integrated PCR-EC microchip format in adapting different EC detection schemes, the intercalator-based approach is replaced with other hybridization transduction methodology. Among the available tech-

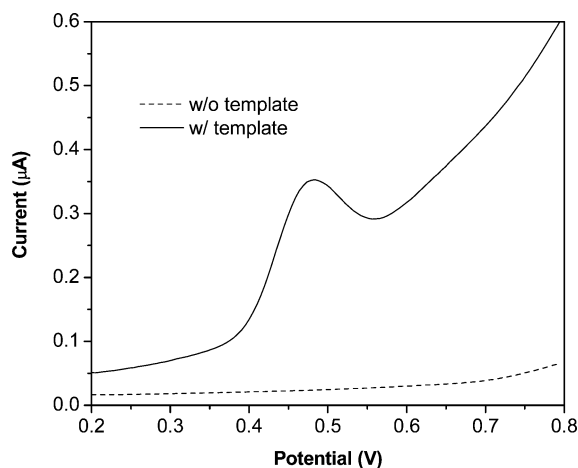


Fig. 3 Differential pulse voltammograms of $100 \mu\text{M}$ Hoechst 33258 intercalated onto the gold working electrodes of the PCR-EC microdevices. The gold electrode, with DNA probe immobilized on its surface, was used to recognize the PCR amplicon (template concentration of $40 \text{ pg } \mu\text{l}^{-1}$) by hybridization when the target was present in the PCR-mix.

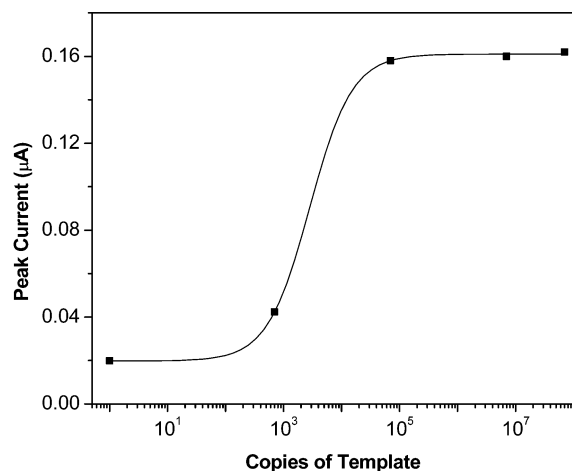


Fig. 4 A calibration plot of the differential pulse voltammetric peak current of the gold working electrode in the PCR-EC microdevice against the number of template molecules in the PCR-mix. The probe-modified gold working electrode was hybridized with the target PCR amplicon and then exposed to $100 \mu\text{M}$ Hoechst 33258 solution. The peak current was calculated by the GPES software with baseline correction.

nologies, the gold nanoparticle-based approach^{35,36} is one of the most promising techniques in EC hybridization transduction attributed to its high sensitivity and selectivity. Unlike the intercalators that bind to the grooves of the double-helical DNA structures, the gold nanoparticle binds to the hybridized amplicon either through interaction between the biotinylated amplicon and the streptavidin-conjugated gold nanoparticle or through a sandwiched assay with another gold nanoparticle-labeled detection probe. Subsequent signal transduction of the hybridization event is achieved by catalytic silver deposition on the gold nanoparticle (termed as silver enhancement), followed by measuring the electrochemical current from the oxidative dissolution of the deposited silver metal. To adopt the silver enhanced gold nanoparticle approach in our PCR-EC microchip setting, electrode material other than gold has to be sought. This is because the gold working electrode has catalytic silver deposition on its surface, resulting in a high background signal that makes the detection of the silver-enhanced gold nanoparticle almost impossible. Indium tin oxide electrode (ITO), with its inherent low background silver deposition characteristic, is an ideal candidate for a sensitive electrochemical detection of the hybridization event with the silver-enhanced gold nanoparticle approach.⁴⁰ To develop a PCR-EC microdevice for DNA analysis with the gold nanoparticle approach, the PCR reaction chamber is sealed with an ITO-coated glass substrate. Similarly to the PCR-EC microchip with gold working electrode, the ITO electrode has to be modified with the probe. In this case, the probe is attached to the silanized ITO surface *via* disulfide-linkage. Fig. 5 shows the enhanced linear sweep voltammetric response of the PCR-EC microdevice using an ITO electrode. It can be seen that the electrochemical signal of silver is much higher for the reaction mixture containing trace amounts of DNA template (~ 700 copies) than that without DNA templates. Similarly as in the case for the intercalator approach using a gold electrode, the signal enhancement here can be explained by the increased deposition of silver on the nanogold particles of the asymmetric PCR amplicons after hybridization with the probe DNA on the silanized ITO surface.

There are numerous potential application areas for the integrated PCR-EC microdevice described here. With the target amplification capability offered by the PCR, this micro-fabricated DNA analyzer holds a great promise for rare target identification in point-of-care genetic diagnostics as well as environmental and food screening applications. This PCR-EC microdevice can be adapted to a multiplexing assay in a single

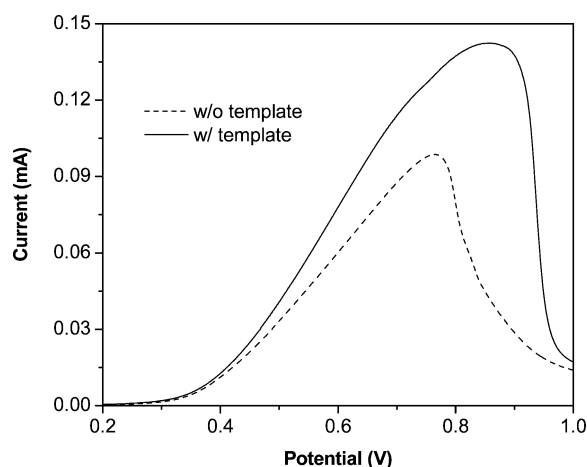


Fig. 5 Linear sweep voltammograms of the indium tin oxide (ITO) working electrodes in the PCR-EC microdevices. The probe-modified ITO electrode was employed to sense the target PCR amplicon (template concentration of $0.4 \text{ fg } \mu\text{l}^{-1}$). The gold nanoparticle was bound to the hybridized amplicon and silver was catalytically deposited onto the nanoparticle.

reaction chamber by constructing an array of working electrodes with different DNA probes.

4 Conclusion

We have developed a silicon/glass-based polymerase chain reaction-electrochemical (PCR-EC) microdevice for DNA analysis with integrated target DNA amplification and product detection functionalities. The microchip had sensors and heaters patterned on top of the silicon reaction chamber for precise and efficient thermal cycling of the PCR. Moreover, the glass substrate was equipped with electrochemical detection electrodes. We have successfully demonstrated the sensitive detection of target DNA template in the PCR-EC microdevice with two electrochemical hybridization transduction schemes: the intercalator-based and silver-enhanced gold nanoparticle-based approaches. With the PCR-EC microchip as the basic framework, in the future, it is hoped that additional features such as sample preparation, microfluidic control, and on-chip/board electronic signal processing functionalities can be integrated onto a monolithic platform to realize a portable DNA analysis system.

Acknowledgements

The authors thank the funding support from the Institute of Integrated Microsystem of the Hong Kong University of Science and Technology (HKUST) (Project No.: I²M/S01/02.EG03) and the Research Grants Council of the Hong Kong Special Administrative Region (Project No.: HKUST 6019/02P). The authors also thank Prof. Karl Tsim of the Department of Biology at HKUST for providing DNA plasmid containing *F. thumbergii* 5S-RNA spacer domains. Laboratory facilities provided by the Biotechnology Research Institute at HKUST are also acknowledged here.

References

- 1 C. H. Mastrangelo, M. A. Burns and D. T. Burke, *Proc. IEEE*, 1998, **86**, 1769–1787.
- 2 S. Abramowitz, *J. Biomed. Microdevices*, 1999, **1**, 107–112.
- 3 D. Trau, T. M. H. Lee, A. I. K. Lao, R. Lenigk, I. M. Hsing, N. Y. Ip, M. C. Carles and N. J. Sucher, *Anal. Chem.*, 2002, **74**, 3168–3173.
- 4 R. C. Anderson, X. Su, G. J. Bogdan and J. Fenton, *Nucleic Acids Res.*, 2000, **28**, e60.
- 5 K. B. Mullis, F. Ferre and R. A. Gibbs, *The Polymerase Chain Reaction*, Birkhauser, Boston, 1994.
- 6 P. Wilding, M. A. Shoffner and L. J. Kricka, *Clin. Chem.*, 1994, **40**, 1815–1818.
- 7 M. A. Shoffner, J. Cheng, G. E. Hvichia, L. J. Kricka and P. Wilding, *Nucleic Acids Res.*, 1996, **24**, 375–379.
- 8 M. A. Northrup, C. Gonzalez, D. Hadley, R. F. Hills, P. Landre, S. Lehw, R. Saiki, J. J. Sninsky, R. Watson and R. Watson Jr., *Dig. Tech. Pap.: Transducers 1995*, 1995, **1**, 764–767.
- 9 T. B. Taylor, E. S. Winn-Deen, E. Picozza, T. M. Woudenberg and M. Albin, *Nucleic Acids Res.*, 1997, **25**, 3164–3168.
- 10 J. H. Daniel, S. Iqbal, R. B. Millington, D. F. Moore, C. R. Lowe, D. L. Leslie, M. A. Lee and M. J. Pearce, *Sens. Actuators, A*, 1998, **71**, 81–88.
- 11 M. U. Kopp, A. J. de Mello and A. Manz, *Science*, 1998, **280**, 1046–1048.
- 12 T. M. H. Lee, I. M. Hsing, A. I. K. Lao and M. C. Carles, *Anal. Chem.*, 2000, **72**, 4242–4247.
- 13 P. Wilding, L. J. Kricka, J. Cheng, G. Hvichia, M. A. Shoffner and P. Fortina, *Anal. Biochem.*, 1998, **257**, 95–100.
- 14 M. A. Northrup, *Anal. Chem.*, 1998, **70**, 918–922.
- 15 P. Belgrader, S. Young, B. Yuan, M. Primeau, C. A. Lee, F. Pourahmadi and M. A. Northrup, *Anal. Chem.*, 2001, **73**, 286–289.
- 16 A. T. Woolley, D. Hadley, P. Landre, A. J. de Mello, R. A. Mathies and M. A. Northrup, *Anal. Chem.*, 1996, **68**, 4081–4086.
- 17 E. T. Lagally, P. C. Simpson and R. A. Mathies, *Sens. Actuators, B*, 2000, **63**, 138–146.
- 18 J. Cheng, L. C. Waters, P. Fortina, G. Hvichia, S. C. Jacobson, J. M. Ramsey, L. J. Kricka and P. Wilding, *Anal. Biochem.*, 1998, **257**, 101–106.
- 19 J. Khandurina, T. E. McKnight, S. C. Jacobson, L. C. Waters, R. S. Foote and J. M. Ramsey, *Anal. Chem.*, 2000, **72**, 2995–3000.
- 20 M. A. Burns, B. N. Johnson, S. N. Brahmasandra, K. Handique, J. R. Webster, M. Krishnan, T. S. Sammarco, P. M. Man, D. Jones, D. Heldsinger, C. H. Mastrangelo and D. T. Burke, *Science*, 1998, **282**.
- 21 Y. He, Y. H. H. Zhang and E. S. Yeung, *J. Chromatogr., A*, 2001, **924**, 271–284.
- 22 N. Zhang, H. Tan and E. S. Yeung, *Anal. Chem.*, 1999, **71**, 1138–1145.
- 23 J. Wang, *Anal. Chim. Acta*, 2002, **469**, 63–71.
- 24 K. M. Millan and S. R. Mikkelsen, *Anal. Chem.*, 1993, **65**, 2317–2323.
- 25 J. Wang, X. Cai, G. Rivas and H. Shiraishi, *Anal. Chim. Acta*, 1996, **326**, 141–147.
- 26 S. O. Kelley, E. M. Boon, J. K. Barton, N. M. Jackson and M. G. Hill, *Nucleic Acids Res.*, 1999, **27**, 4830–4837.
- 27 K. Hashimoto, K. Ito and Y. Ishimori, *Anal. Chem.*, 1994, **66**, 3830–3833.
- 28 T. M. H. Lee and I. M. Hsing, *Anal. Chem.*, 2002, **74**, 5057–5062.
- 29 T. De Lumley-Woodyear, C. N. Campbell, E. Freeman, A. Freeman, G. Georgiou and A. Heller, *Anal. Chem.*, 1999, **71**, 535–538.
- 30 F. Patolsky, E. Katz, A. Bardea and I. Willner, *Langmuir*, 1999, **15**, 3703–3706.
- 31 L. Authier, C. Grossiord and P. Brossier, *Anal. Chem.*, 2001, **73**, 4450–4456.
- 32 J. Wang, D. Xu, A. N. Kawde and R. Polsky, *Anal. Chem.*, 2001, **73**, 5576–5581.
- 33 H. Cai, Y. Xu, N. Zhu, P. He and Y. Fang, *Analyst*, 2002, **127**, 803–808.
- 34 Y. Uto, H. Kondo, M. Abe, T. Suzuki and S. Takenaka, *Anal. Biochem.*, 1997, **250**, 122–124.
- 35 J. Wang, R. Polsky and D. Xu, *Langmuir*, 2001, **17**, 5739–5741.
- 36 H. Cai, Y. Wang, P. He and Y. Fang, *Anal. Chim. Acta*, 2002, **469**, 165–172.
- 37 T. M. H. Lee, I. M. Hsing and C. Y. N. Liaw, *J. Microelectromech. Syst.*, 2000, **9**, 469–473.
- 38 D. E. Seborg, T. F. Edgar and D. A. Mellichamp, *Process Dynamics and Control*, Wiley, New York, 1989, ch. 7 and 12.
- 39 Z. H. Cai, P. Li, T. T. X. Dong and K. W. K. Tsim, *Planta Med.*, 1999, **65**, 360–364.
- 40 T. M. H. Lee, L. L. Li and I. M. Hsing, *Langmuir*, 2003, in press.